

1994012386

N94-16859

**DEVELOPMENT OF BRAIDED FIBER SEALS
FOR ENGINE APPLICATIONS**

Zhong Cai, Rajakkannu Mutharasan, Frank K. Ko, Guang-Wu Du
Drexel University
Philadelphia, PA 19104

Bruce M. Steinetz
NASA Lewis Research Center
Cleveland, OH 44135

ABSTRACT

A new type of braided fiber seal has been developed for high temperature engine applications. Development work performed in this study includes seal design, fabrication, leakage flow testing, and flow resistance modeling. This new type of seal utilizes the high flow resistance of tightly packed fibers and the conformability of textile structures. The seal contains a core part with aligned fibers, and a sheath with braided fiber layers. Seal samples are made by using the conventional braiding process. Leakage flow measurements are then performed. Mass flow rate versus the simulated engine pressure and preload pressure is recorded. The flow resistance of the seal is analyzed using the Ergun equation for flow through porous media, including both laminar and turbulent effects. The two constants in the Ergun equation are evaluated for the seal structures. Leakage flow of the seal under the test condition is found to be in the transition flow region. The analysis is used to predict the leakage flow performance of the seal with the determined design parameters.

INTRODUCTION

The primary design of an engine seal is the prevention of hot engine flow path gases and potentially explosive hydrogen/oxygen mixtures from escaping through the seal and damaging the engine panel support and articulation system. A balanced-pressure seal system with positive purging can be designed which ensures engine flow path gases such as unburned hydrogen do not get behind to movable panels. Because pressure differential across the movable panels is minimized, the pressure loads supported by the seals are greatly reduced. An illustration of the seal application system is shown in Fig. 1. More detailed discussion is given in [1].

The general requirements for the seal system for such applications can be summarized as follows: a) minimize seal leakage; b) conform to and seal against distorted adjacent engine walls; c) operate in a high heat flux environment utilizing minimum coolant resources; d) maintain material stability in a chemically hostile hydrogen-oxygen environment; and e) minimize sliding damage over engine life.

New design concepts have been developed to satisfy the seal performance requirements. One of the choices is to use tightly packed fibers. Textile rope structures have long been used in packing materials and seals. Currently a large family of ceramic fibers is available for applications with high temperature and a hostile environment.

The objective of the current study is to evaluate the leakage performance of a range of braided fiber seal architecture/material configurations. The knowledge acquired through the development work provides a solid data base for various seal applications and for the further improvement of the design and fabrication of seals.

SEAL DESIGN AND FABRICATION

Based on the textile engineering experience, a core-sheath system is selected for the seal structure. This core-sheath structure is made by stuffing tubular fabrics with parallel fiber bundles, as shown in Fig. 1. The structure provides the high capacity for the incorporation of longitudinal fibers. Depending on the fiber architecture selected for the seal system, various levels of conformability, abrasion resistance and packing densities can be developed. Of the wide variety of fiber architectures, braided structures provide the highest level of conformability while maintaining a high level of structural integrity and fiber coverage. Therefore the fabrication process for this core-sheath structure is to braid the sheath on top of the aligned core fibers.

The proposed seal configuration consists of a core part of aligned ceramic fibers and a sleeve with braided ceramic or metallic fibers. In the application the leakage flow is transverse to the aligned fibers. When preload is applied transversely to the seal, these aligned fibers are compacted thus providing very high flow resistance. This design employs the conformability of the fiber structures and also utilizes the high temperature performance of ceramic fibers.

The conventional 2-D braiding method is used for the seal construction. As discussed in [2], 2-D braiding can produce a wide range of braiding angles ($\theta = \pm 10^\circ$ to $\pm 80^\circ$). The physical and mechanical behavior of braided structures depends upon the fiber orientation, fiber properties and fiber volume fraction. The governing equations for 2-D braiding are

$$d_o = \frac{N_{ys} A_{ys}}{\pi t_s V_{fs} \cos \theta} + t_s \quad (1)$$

$$d_i = \frac{N_{ys} A_{ys}}{\pi t_s V_{fs} \cos \theta} - t_s \quad (2)$$

$$d_o - d_i = 2 t_s \quad (3)$$

where d_o is the outside braid diameter, d_i is the inside braid diameter, t_s is the sheath thickness and usually t_s is much smaller than d_i and d_o . N_{ys} is the number of yarns in the sheath, A_{ys} is the nominal yarn cross sectional area along the yarn axis, and V_{fs} is the fiber volume fraction of the sheath. The number of yarns is related to the carrier number N_r , the sheath layer number N_L , and the number of yarns or plies on each carrier N_{yr} as

$$N_{ys} = N_r N_{yr} N_L \quad (4)$$

N_L is also the number of braiding passes in the operation.

As shown in Fig. 1, before installation or after braiding, the seal cross section is in a circular shape. After installation the seal shape becomes close to a rectangle. The dimensions of the rectangle are set by the application requirements. We assume the seal

width and height after the installation are w_s and h_s respectively; the area relation can be expressed approximately as

$$h_s w_s = \pi d_o^2 / 4 \quad (5)$$

From this relation, the nominal seal diameter d_o can be determined. If the yarn number and yarn cross section area in the core N_{yc} and A_{yc} are chosen, the overall porosity of the seal is

$$\epsilon = 1 - V_f = 1 - \frac{N_{yc} A_{yc} + N_{ys} A_{ys} / \cos \theta}{\pi d_o^2 / 4} \quad (6)$$

The relation for the core fiber volume fraction V_{fc} is

$$N_{yc} A_{yc} = V_{fc} (\pi d_i^2 / 4) \quad (7)$$

The sheath layer thickness t_s is related to the braiding operation parameters, such as braiding angle, yarn tension, and sheath layer number. Usually t_s needs to be estimated empirically. The other important seal design parameter, the core percentage of the fiber volume, can be calculated as

$$V_c = \frac{A_{fc}}{A_{ft}} = \frac{A_{fc}}{A_{fs} + A_{fc}} \quad (8)$$

where A_{fc} and A_{fs} are the fiber cross section area along the seal axis for the core and the sheath respectively, and can be calculated as

$$A_{fc} = N_{yc} A_{yc} \quad (9)$$

$$A_{fs} = N_{ys} A_{ys} / \cos \theta \quad (10)$$

We should emphasize that all the calculations involved above are for the nominal values only. Since the yarn size changes during the braiding operation, the final dimension of the seal may vary depending on the fabrication conditions.

LEAKAGE FLOW ANALYSIS

The problem of flow through porous media can be described by the Ergun equation [3, 4]. The differential form of the Ergun equation is

$$-\frac{dp}{dx} = C_L \frac{\mu q (1 - \epsilon)^2}{D_p^2 \epsilon^3} + C_T \frac{\rho q^2 (1 - \epsilon)}{D_p \epsilon^3} \quad (11)$$

where p , μ , and ρ are fluid pressure, viscosity, and density respectively, q is the average flow rate, ϵ is porosity of the medium, and D_p is the characteristic particle dimension. The two dimensionless constants C_L and C_T account for the viscous and turbulent effect respectively, and are determined semi-empirically. For the packed spherical particles, D_p is chosen as the sphere diameter, and C_L and C_T are found to be 150 and 1.75 respectively.

If the viscous flow is dominant, the turbulent flow term can be dropped. This leads to the well-known Kozeny-Carman equation for the laminar flow through porous media. The constant after some conversion becomes the Kozeny constant. However, a large number of experiments show that the constant term varies in different situations, and generally is lower than that in the Ergun equation [5, 6].

Viscous flow through aligned fiber bundles has also been studied in the composite processing field [7, 8, 9, 10]. For aligned fiber bundles, the permeability is not isotropic. The flow resistance in the transverse direction is much higher than that in the longitudinal direction [7, 8, 9]. Also in the transverse direction, flow can stop at the maximum packing efficiency which is less than one [10]. The stop-flow phenomenon is in general not true for other packed beds. Therefore, the Ergun equation or the Kozeny-Carman equation cannot predict this stop-flow behavior. However, in the middle range of the porosity or fiber volume fraction, the Kozeny-Carman equation has been used to give reasonable predictions. Estimations of the Kozeny constant for the longitudinal and transverse flow are presented in [7, 8, 9].

In applying the Ergun equation here, we choose the fiber diameter d_f as the characteristic length to replace D_p . The conversion factor from D_p to d_f is left in the two constants C_L and C_T . For flow through seal structure including packed aligned fibers in the core and braided fiber sheath, we expect C_L and C_T to be different from those in the original Ergun equation [3, 4] because of the geometry configuration. In the seal application, only part of the seal section is exposed to the flow path, as shown in Fig. 1. This will also affect the magnitude of C_L and C_T .

We can also write the flow equation using the form of Darcy's law as

$$-\frac{dp}{dz} = q \frac{\mu}{K} \quad (12)$$

where K is the permeability which has the units of length squared, and z is used for the transverse flow. Alternatively the flow resistance R can be used as

$$-\frac{dp}{dz} = q \mu R \quad (13)$$

where R has the units of one over length squared and is defined as

$$R = (C_L + C_T \text{Re}) \frac{1}{d_f^2} \frac{(1 - \epsilon)^2}{\epsilon^3} = \frac{C_L}{d_f^2} \frac{(1 - \epsilon)^2}{\epsilon^3} \left(1 + \text{Re} \frac{C_T}{C_L} \right) \quad (14)$$

where the Reynolds number Re for the flow is defined as

$$\text{Re} = \frac{\dot{m} d_f}{\mu (1 - \epsilon)} = \frac{\rho q d_f}{\mu (1 - \epsilon)} \quad (15)$$

The mass flow rate \dot{m} is calculated using the seal cross section area transverse to the flow, and is a constant over the flow length. In the viscous flow case, this flow resistance R is only a function of the fibrous structure which is represented by d_f , ϵ , and C_L . However, if the turbulent flow cannot be neglected, then the fluid property and the velocity also enter the expression through Re .

From the above discussion, it is clear that in the seal design, both the porosity and the fiber diameter strongly influence the flow resistance. Also with the turbulent effect, the overall seal resistance is increased.

To solve for the seal leakage rate, we applied the ideal gas law for the relation between ρ and p as

$$\rho = \frac{M_w}{R_g T} p = \frac{p_o}{p_o} p \quad (16)$$

where M_w is the molecular weight, R_g is the gas constant, T is the temperature, and ρ_o and p_o are the reference values at the temperature. The viscosity of the gas is considered to be constant over the seal length for the simplification of the problem. By applying these relations and rearranging various terms, we can obtain

$$C_L \left[\frac{\mu (1 - \epsilon)}{d_f \dot{m}} \right] + C_T = \frac{1}{2} \frac{p_{in}^2 - p_{out}^2}{w_s} \frac{\rho_o}{p_o} \frac{d_f}{\dot{m}^2} \frac{\epsilon^3}{(1 - \epsilon)} \quad (17)$$

where subscripts *in* and *out* indicate the inlet and outlet locations of the seal respectively, w_s is the seal width after installation, and the engine pressure $p_e = p_{in} - p_{out}$.

With this leakage flow equation, we can set up experiments to measure the leakage mass flux versus the engine pressure, then evaluate the unknown constant terms C_L and C_T for the designed seal structure. Since the leakage flow equation is in the linear form for C_L and C_T , a linear regression of the test data can be conveniently performed. After we obtained these constant values, the seal leakage rate under the application conditions can be predicted.

LEAKAGE FLOW TEST

Leakage test setup is illustrated in Fig. 2. Flow media included air and helium since they represent different transport properties. Engine pressure p_e was simulated using the compressed gases, and was regulated using a series of valves. The seal was placed into a groove of 0.5 inch (0.0127 m) wide in the lower platen of the test fixture. An expandable soft-tube bladder was inserted at the bottom of the groove. This bladder tube was connected to another compressed air line, and the pressure in this line was also regulated. In the test this line pressure, which was the preload pressure p_p for the seal, was set at different levels, typically 20, 40, 80, and 130 psig (0.138, 0.276, 0.552, and 0.896 MPa) respectively. When the bladder tube was pressurized, it pushed the seal upwards against the top plate. A gasket was installed between the top plate and the bottom part of the fixture to ensure that leakage occurred only through the seal. The seal sealed an inter-panel gap that was 4 inch (0.102 m) long and 0.2 inch (0.0508 m) high.

The measurement devices include a digital pressure gage, Model PX-623, a pressure conditioner, Model DP41-V-A, a mass flow meter, Model FMA-875-V, and a conditioner, Model FMA-78P2, all of them from Omega Engineering. The mass flow meter was connected to the gas input line. The pressure gage was positioned at the inlet side of the seal. The outlet pressure was atmospheric pressure. Therefore the recorded pressure difference was used to simulate the engine pressure.

In the leakage test, seals are carefully placed into the groove. After that the top plate was installed. Preload pressure of 130 psi (0.896 MPa) was first applied to consolidate the seal structure. This preload pressure was maintained for about a minute, and then released. This was to ensure the consistency of the initial test condition of the seal. Then the flow gas, either helium or air, was introduced. A regulator on the gas input line was used as the control device to obtain the desired engine pressure values. After the readings reached the steady state (usually in less than a minute), the mass flow rate was recorded. The simulated engine pressure was increased from 0 to 50 psig (0.345 MPa), and maintained at a series of preset values for the reading. Because the mass flow meter can handle about 200 liters per minute maximum flow rate, for some seals the maximum pressure values were lower than 50 psig (0.345 MPa). Tests were first done at the lower preload pressure values, for example, 20 psig (0.138 MPa), and then increased to the next higher level. A systematic application of preload was used to eliminate the potential hysteresis effects in the measurement. When tests at various preload levels were completed, preload line pressure was released. The seal sample was then taken out of the apparatus, and the dimensions of the seal were measured at five locations along the seal length using a caliper.

SEAL PERFORMANCE

The effect of the main design parameters, such as fiber diameter, braiding angle, sheath layer number, and seal porosity, on the seal leakage performance has been observed in the seal leakage tests. As discussed earlier, seal porosity and fiber diameter showed great influence in the overall seal leakage performance.

Sample to sample variation of the seal leakage rate was one of the main concerns of the seal performance. In the fabrication process, a long braided structure was made, then seal samples with 5.6 inch (0.142 m) lengths were cut from the long structure. Theoretically, these seal samples had the same porosity and fiber architecture. The variation among different seal samples with the same structure reflected the influence of random operating conditions in the fabrication process, which is not unusual in the textile process. The variation is important to the quality control of the seal performance.

Fig. 3 shows the mass flow rate of four seals M1-(1) to M1-(4) under the preload pressures 40 psi (0.276 MPa). Data of both air and helium is included. The results show that the variation among these seal samples is relatively small, with readings within $\pm 15\%$ of the sample average. The variation was also checked for the eight seals of batch M1. At the preload $p_p=40$ psig (0.276 MPa) and the engine pressure $p_e=5$ psig (0.0345 MPa) with helium as the medium, the mass flow rate of the sample average is 0.00196 (lb/ft/sec), and the standard deviation is 0.00024 (lb/ft/sec).

The other variation checked is in the measurement of the flow leakage test. This was performed on the M6c batch seals. Each sample was measured three times. The consecutive measurements were made after the seal was taken out of the test fixture for at least 24 hours, allowing the seal to essentially return to its initial condition. Sample average and variance were calculated. A flow parameter is used which is defined as the mass flow rate of helium per second per foot of seal multiplied by the square root of the absolute temperature, divided by the absolute inlet pressure. This flow parameter has the units of $[\text{lb (He) } ^\circ\text{R}^{1/2}]/[\text{s ft psia}]$. The test condition is set at the preload pressure of 40 psig and engine pressure of 15 psig. The sample average of the flow parameter of M6c-(1) seal is 0.001290 and the sample variance is 0.000025. Correspondingly these values of sample M6c-(2) are 0.001166 and 0.000054 respectively. These results show that the variation of the measurement is acceptable.

A typical response of the seals using the permeability versus the applied preload p_p and the simulated engine pressure p_e is shown in Fig. 4. The seal permeability decreases when the engine pressure or the preload pressure increases. It appears that the effect of the engine pressure on the permeability is stronger than that of the preload pressure. As we discussed in the previous section, the seal structure Re was controlled by p_e which determined the mass flow rate. The turbulent part of the flow resistance is therefore strongly related to p_e . The viscous flow resistance was greatly influenced by the seal porosity which is related to the preload p_p . In the case of relatively high fiber volume fractions, which was true for the seal design, applying p_p can only change the porosity to a very limited extent. When p_e was increased during the flow leakage test, the change of Re was significant.

To determine the seal response to the transverse preload pressure, another experimental measurement was conducted, in which an Instron machine was used to compress the seal placed into a mold with the same dimensions as the leakage flow test device. Both the deflection and the load were monitored. Load was applied up to 1100 lbf (500 kg), for the seal sample of about 5.6 inch (0.142 m) length. Seal porosity was determined using the measured mold height and the nominal fiber content.

Since seals were designed with different parameters, such as fiber content, core percentage, braiding angle, and fiber type, the load-deflection responses of these seals were very different. However, they all showed nonlinear response as other fibrous preforms reported in the literature [9-15]. A comparison of the seal response with the available fiber deflection model proposed in [14] is shown in Fig. 5. A good agreement can be seen for most part of the fiber volume fraction range.

LEAKAGE FLOW MODELING

To determine the constants C_L and C_T for the designed seal structure, leakage flow test data was used. As we mentioned above, if the measurements are taken correctly, and the Ergun equation is valid, then the values of C_L and C_T will be constant for a specific seal sample under the test condition. Also the leakage flow equation has the form of $y = ax+b$, with x and y defined as

$$x = \frac{\mu (1 - \epsilon)}{d_f \dot{m}} = \frac{1}{Re} \quad (18)$$

$$y = \frac{1}{2} \frac{p_{in}^2 - p_{out}^2}{w_s} \frac{\rho_o}{p_o} \frac{d_f}{\dot{m}^2} \frac{\epsilon^3}{(1 - \epsilon)} \quad (19)$$

and the equation becomes

$$y = C_L x + C_T \quad (20)$$

The measurement data of different gases, helium and air, will then fall on one straight line. The values of these two constants can also be determined using the linear regression approach.

Fig. 6 shows two selected seal samples using the x - y plot. Although there are data scattering in the figure, it is reasonable to conclude that the Ergun equation is valid for the seal leakage flow. The constant values of C_L and C_T for these two seals are 3.4 and 4.4 for M2-(1), and 85 and 170 for M5-(1) respectively, using the least square regression for each test batch and averaged value for the seal sample. The correlation coefficient of the linear

regression in most cases is larger than 0.99. However, variations of C_L and C_T under different preloads can also be seen in Fig. 6. The overall seal performance is still related to other parameters, such as fiber diameter or porosity. If other parameters are all the same, then the higher the values of C_L and C_T are, the higher the seal resistance is.

The ratio of C_T/C_L is also important in evaluating the turbulent effect of the leakage flow process. As we discussed earlier, the seal resistance is the summation of the laminar and turbulent flow resistances. The relative magnitude of the turbulent effect can be determined using the index $Re \cdot (C_T/C_L)$, not just Re . In the original Ergun equation [3, 4], with the given values of $C_L=150$ and $C_T=1.75$, the requirement to neglect the turbulent effect is that $Re < 10$. In the seal structure and test setup, the values of C_L and C_T were significantly different. Therefore $Re < 10$ was no longer a valid criterion in determining whether the turbulent flow was negligible. As shown in equation (14), the contribution of the turbulence effect to the flow resistance can be measured by the term $Re \cdot (C_T/C_L)$. Therefore the correct criterion should be $Re \cdot (C_T/C_L) \ll 1$. The ratio of C_T/C_L for most of the seal samples was found to be at the range of 1 to 2 from experiments. Therefore the corresponding requirement for Re is $Re < 0.1$, which is much more severe than other cases.

In the leakage flow test, the range of Re was found to be between 0.1 to 5. Therefore, the flow is in the transition region. The ratio of mass flow rate of air to helium was used to check the flow status. The theoretical value of this ratio for laminar flow is

$(\mu/\rho)_{\text{helium}}/(\mu/\rho)_{\text{air}} = 7.86$, and that of turbulent flow is $(\rho_{\text{air}}/\rho_{\text{helium}})^{1/2} = 2.69$. This ratio of all the seals tested was in the range of 3 to 7.

SUMMARY

The work performed in this study showed that the application of braided fiber seal is feasible. Seals were designed and fabricated using different fiber architectures, and then tested for the leakage flow. It was found that many design parameters, such as the seal porosity, the percentage of the core part, layer number of the sheath, fiber diameter, sheath braiding angle, and sheath thickness, all contribute to the seal leakage performance. Qualitative relationships have been established between the design parameters and seal performance.

The Ergun equation is applied to the leakage flow analysis. The two constants in the Ergun equation, C_L and C_T which accounted for laminar and turbulent effects respectively, are found to be substantially different from those suggested in the literature for other packed geometries. Test data show that C_L and C_T have about the same order for the seal structure and the flow leakage test setup. The relative magnitude of the turbulent effect versus laminar effect can be correctly evaluated using an index $(Re \cdot C_T/C_L)$, not just Re . In the seal leakage flow case this leads to a conclusion that only if Re is less than 0.1 or so, can the turbulent effect be neglected. The leakage flow of the seal under the test condition was found to be in the transition region.

ACKNOWLEDGEMENT

The authors would like to thank Hon Wong, Dan Luu, John McKelvie, and Tim Tezak of Drexel University for their help in the seal design, fabrication, and testing, and Christopher Pastore, Susan Marr and Xiaoming Tao for their work in the preliminary design experiments. The project funding by NASA Lewis Research Center is gratefully acknowledged.

REFERENCES

1. Steinetz, B.M., DellaCorte, C., and Sirocky, P.J., "On the Development of Hypersonic Engine Seals", NASA TP-2854, 1988.
2. Ko, F.K., "Braiding", Engineering Materials Handbook, Vol. 1, Composites, Edited by Reinhart, T.J., American Society for Materials International, Metal Park, OH, 1988.
3. Bird, R.B., Stewart, W.E., and Lightfoot, E.N., Transport Phenomena, John Wiley & Sons, 1960, pp.181-200.
4. Denn, M.M., Process Fluid Mechanics, Prentice-Hall, 1980, pp.67-71.
5. Carman, P.C., Flow of Gases through Porous Media, Academic Press, 1956.
6. Van Den Brekel, L.D., and De Long, E.J., "Hydrodynamics in Packed Textile Beds", *Textile Research Journal*, August, 1989, pp.433-440.
7. Williams, J.G., Morris, C.E.M., and Ennis, B.C., "Liquid Flow Through Aligned Fiber Beds", *Polymer Engineering and Science*, Vol. 14, No. 6, June, 1974, pp.413-419.
8. Lam, R.C. and Kardos, J.L., "The Permeability of Aligned and Cross-Plied Fiber Beds During Processing of Continuous Fiber Composites", Proceedings of American Society for Composites, Third Technical Conference, Seattle, Washington, September, 1988, pp.3-11.
9. Lam, R.C. and Kardos, J.L., "The Permeability and Compressibility of Aligned and Cross-Plied Carbon Fiber Beds During Processing of Composites", Proceedings of 47th Annual Technical Conference (ANTEC'89), SPE, New York, 1989, pp.1408-1412.
10. Gutowski, T.G., et. al., "Consolidation Experiments for Laminate Composites", *Journal of Composite Materials*, Vol. 21, June, 1987, pp.650-669.
11. van Wyk, C.M., "Note on the Compressibility of Wool", *Journal of Textile Institute*, Vol. 37, 1946, T285-292.
12. Dunlop, J.I., "On the Compression Characteristics of Fiber Masses", *Journal of Textile Institute*, Vol. 74, 1983, pp.92-97.
13. Carnaby, G.A. and Pan, N., "Theory of the Compression Hysteresis of Fibrous Assemblies", *Textile Research Journal*, Vol. 59, 1989, pp.275-284.
14. Gutowski, T.G., Morigaki, T., and Cai, Z., "The Consolidation of Laminate Composites", *Journal of Composite Materials*, Vol. 21, February 1987.
15. Kim, Y.R., McCarthy, S.P., and Fanucci, J.P., "Compressibility and Relaxation of Fiber Reinforcements During Composite Processing", *Polymer Composites*, Vol. 12, No. 1, February 1991, pp.13-19.

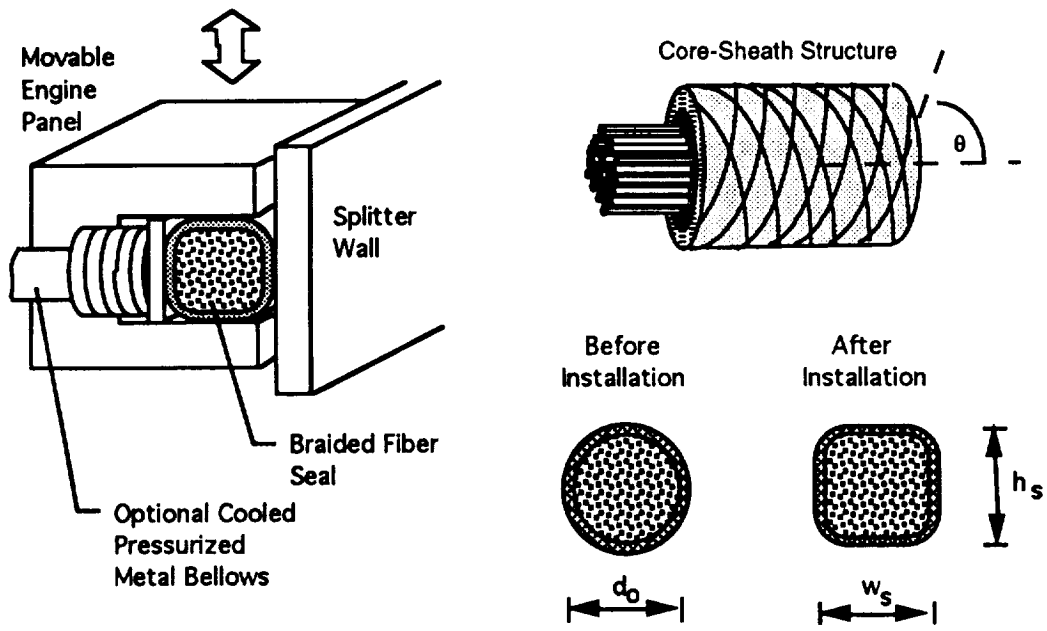


Fig. 1: Illustration of the seal structure and applications.

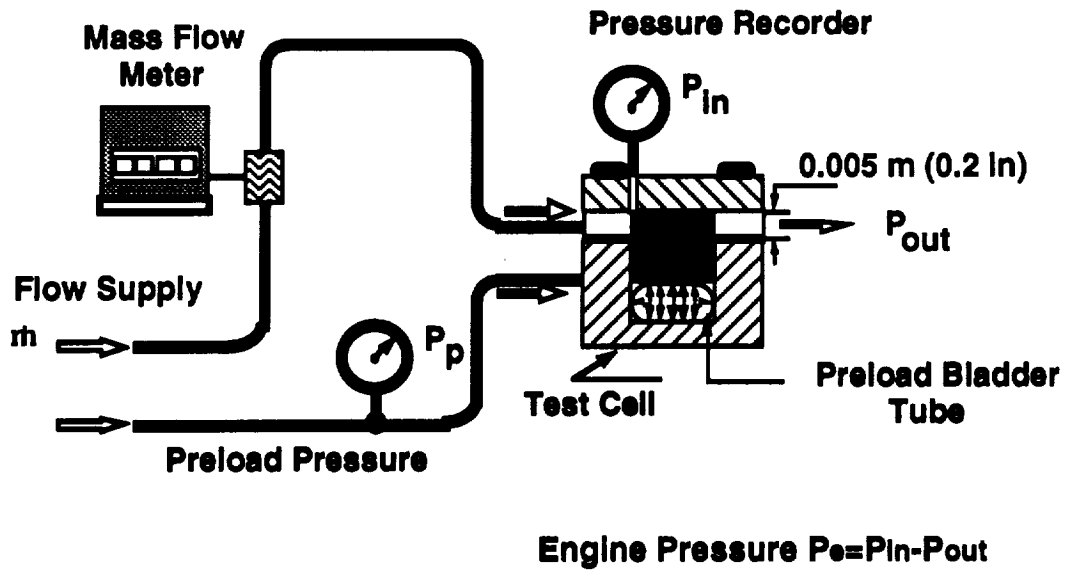


Fig. 2: Leakage flow test setup.

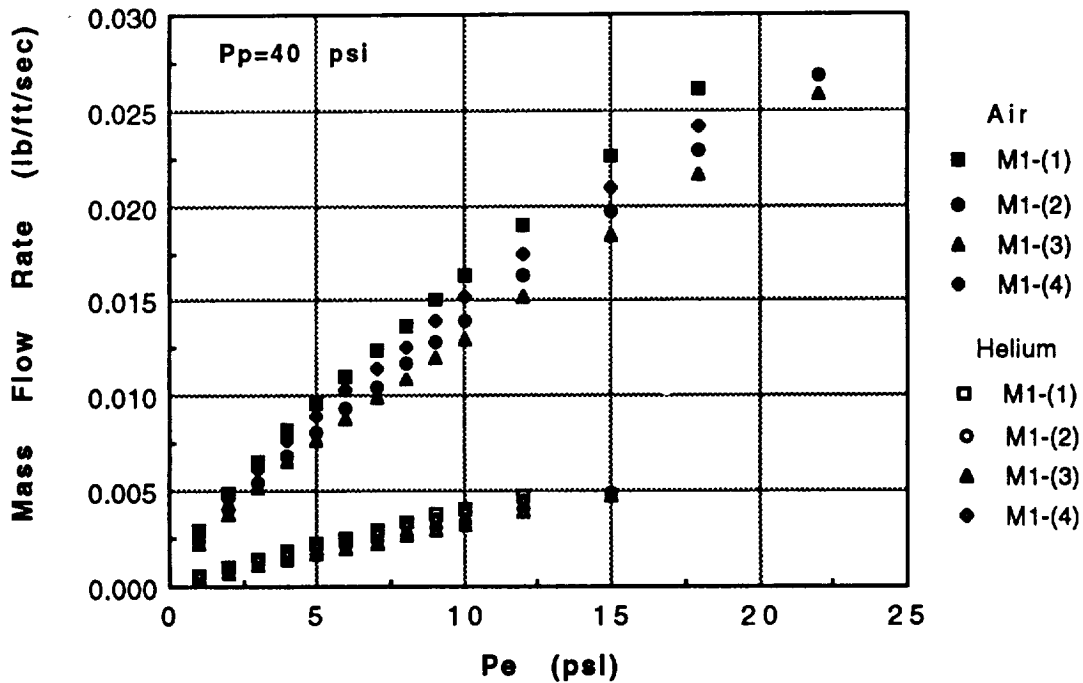


Fig. 3: Variation among the same batch of seal samples.

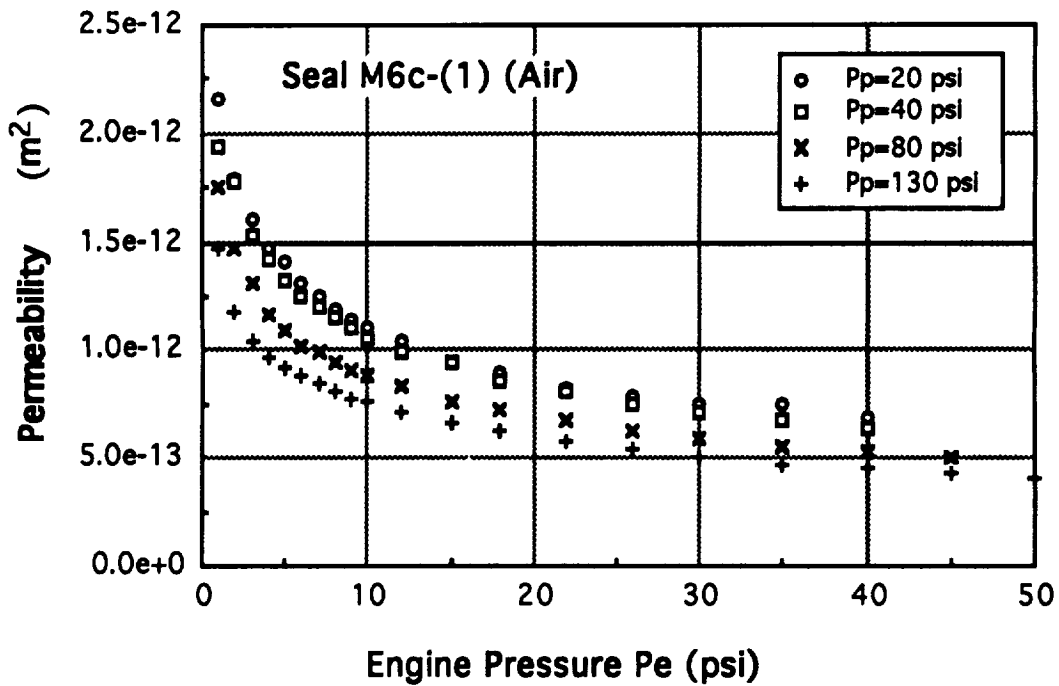


Fig. 4: Permeability versus the engine pressure p_e and the preload p_p .

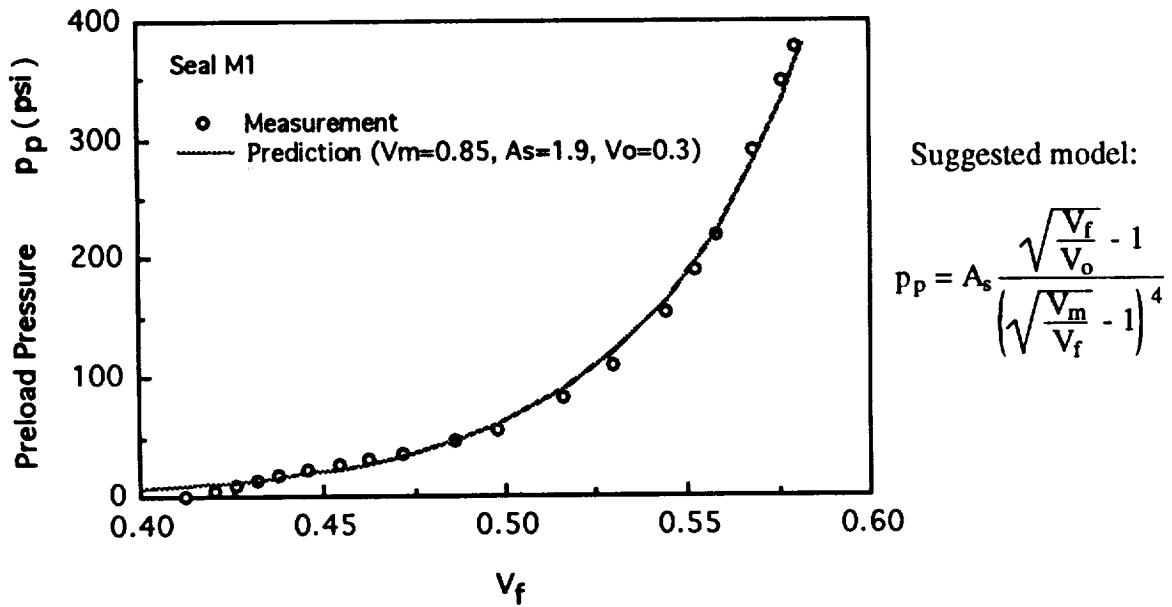


Fig. 5: Comparison of test data and model prediction [14] on seal porosity.

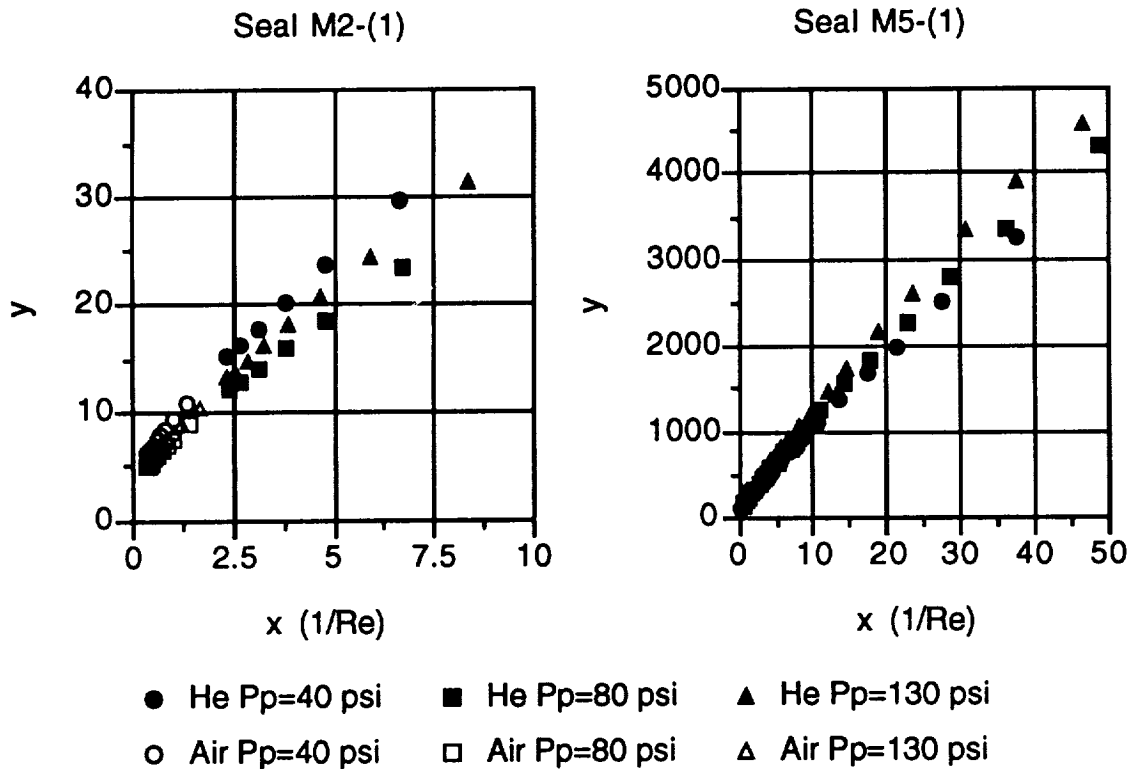


Fig. 6: Flow test data using dimensionless variables.